

Source Analysis of Median Nerve Stimulated Somatosensory Evoked Potentials and Fields Using Simultaneously Measured EEG and MEG Signals.

Mideksa, K.G., Hellriegel, H., Hoogenboom, N., Krause, H., Schnitzler, A., Deuschl, G., Raethjen, J., Heute, U., and Muthuraman, M.

Abstract—The sources of somatosensory evoked potentials (SEPs) and fields (SEFs), which is a standard paradigm, is investigated using multichannel EEG and MEG simultaneous recordings. The hypothesis that SEP & SEF sources are generated in the posterior bank of the central sulcus is tested, and analyses are compared based on EEG only, MEG only, band-pass filtered MEG, and both combined. To locate the sources, the forward problem is first solved by using the boundary-element method for realistic head models and by using a locally-fitted-sphere approach for averaged head models consisting of a set of connected volumes, typically representing the skull, scalp, and brain. The location of each dipole is then estimated using fixed MUSIC and current-density-reconstruction (CDR) algorithms. For both analyses, the results demonstrate that the band-pass filtered MEG can localize the sources accurately at the desired region as compared to only EEG and unfiltered MEG. For CDR analysis, it looks like MEG affects EEG during the combined analyses. The MUSIC algorithm gives better results than CDR, and when comparing the two head models, the averaged and the realistic head models showed the same result.

I. INTRODUCTION

The current sources of electrically stimulated somatosensory evoked potentials (SEPs) following the median-nerve stimulation have been reported in a large number of papers [e.g., 1-3]. Recently, multichannel simultaneous measurements of both electric potentials, which provide information about the entire activity of the brain, including deep and radially oriented sources, and magnetic fields, which provide the most accurate localization of tangentially oriented, superficially located sources, are used to record SEPs and somatosensory evoked fields (SEFs), respectively. The combination of both technologies with 3D magnetic-resonance imaging (MRI) yields further information that helps in separation and localization of focal brain activity.

*Research supported by SFB 855 Project D2.

K.G. Mideksa, H. Hellriegel, G. Deuschl, J. Raethjen, M. Muthuraman are with the Department of Neurology, Christian Albrechts university Kiel, 24105 Germany kgm at tf.uni-kiel.de, h.hellriegel at neurologie.uni-kiel.de, g.deuschl at neurologie.uni-kiel.de, j.raethjen at neurologie.uni-kiel.de, m.muthuraman at neurologie.uni-kiel.de

N. Hoogenboom, H. Krause, A. Schnitzler are with the Department of Neurology, Heinrich-Heine University Duesseldorf, 40225 Germany Nienke.Hoogenboom at med.uni-duesseldorf.de, Holger.Krause at uni-duesseldorf.de, schnitza at uni-duesseldorf.de

U. Heute is with the Institute for Circuit and System Theory, Faculty of Engineering, Christian-Albrechts-University of Kiel, 24105 Germany uh at tf.uni-kiel.de

In order to locate the source for the specific activity seen on the scalp, two problems need to be solved which are the forward and the inverse problem. Finding the rules of the signal propagation is the first step in every source-analysis approach and is termed the 'forward problem' [4]. This problem involves calculating the electric potentials or magnetic fields generated by known current sources for a given head model. Two head models are used: spherical and realistic head geometries. Depending on the geometry assumed for the volume-conductor model, the approaches that lead to a solution for the forward problem are either numerical or analytical [5]. Analytical solutions exist for simplified geometries, e. g., if the head is assumed to consist of a set of nested concentric homogeneous spherical shells representing the skull, scalp, and brain. The forward EEG and MEG problem can then be solved by approximating the skull using a locally fitted sphere, for which closed-form solutions exist [6]. In this case, the forward EEG and MEG problem can be solved numerically using a boundary-element method (BEM). In the second step, signal-processing techniques are applied to solve the 'inverse problem' [7], that is, to estimate the current sources inside the brain that best fit the measured data. In our work, we used two approaches, which apply certain constraints to obtain a unique solution. The most common approach used is the dipole model, each active brain region being modeled with at least one point-like dipole with its position and orientation being fixed. Instead of point-like sources, the other approach, the distributed-source or current-density model, searches for the best estimate of a distributed primary current and is known as the minimum-norm algorithm, where the solution with the smallest norm is selected from all those current distributions that could explain the measured potential or magnetic field [8].

Thus, these two approaches based on realistic (using the individual MRI and known individual electrode locations from each of the subjects) and averaged (contained in the CURRY software) head models is tested, using only EEG, only MEG, band-pass filtered MEG, and both combined.

II. DATA ACQUISITION

Simultaneous EEG and MEG recording and storage of the data to a single file, taken from five healthy subjects, was done using the Elekta Neuromag system. The EEG data were recorded with 128 electrodes, the MEG data from 306 sensors consisting of a triple sensor array, which optimally

combines the focal sensitivity of 204 planar gradiometers and the widespread sensitivity of 102 magnetometers.

The right median nerve was stimulated at the wrist by placing the anode between the tendons of the palmaris longus muscle to record SEPs & SEFs. The nerve was stimulated 200 times with the interval of approximately 300ms between each stimulus. The stimulus intensity was set high enough to produce a consistent muscle twitch, which usually is tolerable by the subject. The recording lasts for 2 minutes for each subject. The EEG, band-pass filtered between 0.01 and 200Hz, and MEG signals were sampled at 1000Hz.

III. METHODS

Since SEPs & SEFs are typically not visible in the raw data recorded from the surface electrodes, signal averaging is used to extract the SEPs & SEFs picked up by the recording electrodes. After being averaged, the most predominant peak is observed in EEG and MEG signals known as N20 which refers to a negative peak (N) at 20 ms after the median nerve is stimulated. The stimulated signal reaches the somatosensory cortex with a delay of 20 ms.

To reconstruct the N20-peak generators, first, the realistic volume-conductor head model, consisting of three layers with conductivity values 0.33, 0.0042, and 0.33S/m for the brain, skull, and scalp, respectively, was constructed by BEM for each subject. The surfaces required for computation of the forward solution (boundaries of scalp, brain-skull, skull-scalp, and cortical surface within the head) were automatically determined from individual MRIs using a segmentation technique by setting a threshold value in such a way that the boundaries separating the tissues from each other do not overlap. The second head model is the averaged head model.

The resulting forward model is then used to solve the inverse problem. Dipole source analysis (fixed MUSIC) and the minimum-norm estimate (MNE) from CDR algorithms and standardized low-resolution brain electromagnetic tomography (sLORETA) are used to reconstruct the N20-peak.

A. Fixed MUSIC

A parametric approach, which requires an explicit a-priori assumption about the cerebral current sources, is termed "fixed MUSIC". Parametric-optimization methods are also known as equivalent current-dipole (ECD) methods or spatio-temporal dipole-fit models. The final result is highly dependent on the initial assumptions regarding the number of dipoles to estimate the sources. In this approach, the fitting procedure leads to an over-determined system of equations since the number of unknown dipole parameters is less than the number of electrodes and sensors. Thus, to estimate the optimal number of dipoles, different optimization algorithms are proposed in [7]. Here, the spatio-temporal decomposition approach based on principal and independent-component analysis (PCA/ICA) is used for defining the source space and estimating the minimum number of dipoles.

MUSIC is a scanning method which does not compute the misfit of a given dipole model per location as in the case of least-squares estimation, but a specific MUSIC

metric, namely, the signal subspace. A signal subspace is first estimated from the data by finding the singular value decomposition (SVD) [9].

$$\mathbf{M} = \mathbf{U}\Sigma\mathbf{R}^T \quad (1)$$

The signal subspace is associated with the leading singular values of the spatio-temporal measured ($m \times n$) data matrix \mathbf{M} for m channels and n time points. \mathbf{U} stands for the subspace orthogonal to the signal subspace which is associated with the trailing singular values of \mathbf{M} and \mathbf{R}^T is the rotational component of the dipole. The number of singular values that make up the signal subspace is a parameter for this method. The MUSIC algorithm then scans a single dipole model through the head volume and computes projections onto this subspace. The MUSIC cost function to be minimized is:

$$\frac{\|\mathbf{N}_s^\perp \mathbf{f}(\mathbf{r}, \mathbf{e})\|^2}{\|\mathbf{f}(\mathbf{r}, \mathbf{e})\|^2} \quad (2)$$

Here, $\mathbf{N}_s^\perp = \mathbf{I} - (\mathbf{U}_s \mathbf{U}_s^T)$ is the orthogonal projector onto the noise subspace with \mathbf{U}_s being the signal subspace spanned by the first left-singular vectors of \mathbf{U} , $\mathbf{f}(\mathbf{r}, \mathbf{e})$ is a function consisting of \mathbf{r} , location and \mathbf{e} , orientation vectors. This cost function is zero when $\mathbf{f}(\mathbf{r}, \mathbf{e})$ is equivalent to one of the true source locations and orientations.

An advantage over least-squares estimation is that each source is found one by one, rather than searching simultaneously for all sources. The MUSIC algorithm gives the best results for temporarily independent sources with fixed orientations (e.g., SEPs) [10].

The drawback of the ECD approach is that it is not possible to localize extended or distributed sources. This gives rise to distributed source models.

B. Minimum Norm Estimate

An increasing interest in current-density reconstruction algorithms has occurred during the past few years. All these algorithms have in common that elementary dipoles are distributed on regular grids inside the head or in cortically constrained implementations on the gray-matter layer [11]. The calculation of the strengths and orientations of these dipoles usually leads to a highly under-determined system of equations - the number of unknown dipole components are greater than the number of electrodes and sensors. Thus, it requires additional mathematical constraints (e.g., minimum-norm and variance-weighted minimum-norm) to yield unique solutions.

A generalized formulation for the minimum-norm solution of the inverse problem with a squared deviation, Δ^2 , and the dipole component vector, \mathbf{j} , can be written as follows:

$$\Delta^2 = |\mathbf{D}(\mathbf{M} - \mathbf{L}\mathbf{j})|^2 + \lambda^2 |\mathbf{C}\mathbf{j}|^2 \quad (3)$$

The data term, $|\mathbf{D}(\mathbf{M} - \mathbf{L}\mathbf{j})|^2$, (measuring the closeness of the obtained solution to the data) and the constraining model term, $\mathbf{M}(\mathbf{j})$, (measuring the closeness to a given

source model) are optimized simultaneously. Both are linked using a regularization parameter, λ . \mathbf{M} is the spatiotemporal measured data matrix ($m \times n$), lead-field matrix \mathbf{L} ($m \times c$ current dipole components), \mathbf{D} is an ($m \times m$) weighting matrix of the sensors, and \mathbf{C} is a ($c \times c$) weighting matrix of the current dipole components. CURRY offers the goodness-of-fit ($1/\text{SNR}$) criterion for determining the optimal value of the regularization parameter so that no overfitting or underfitting of the data occurs. Thus, within the minimum-norm least-squares (MNLS) framework, the solution that has the minimum power is chosen from the non-unique solution set. This standard solution is known to generate very smooth solutions and favors superficial source distributions, even if the true source is a deeper, more focal, current generator. This is due to the reason that small currents close to the detectors can produce fields of similar strengths as larger currents at greater depths. To compensate for the undesired depth dependency of this approach, the currents can be weighted to account for the lower gains of deeper dipole components (lead-field normalization) which leads to the second method known as sLORETA.

C. Standardized Low-Resolution Brain Electromagnetic Tomography

sLORETA is a method in which localization is based on images of standardized current density. It is a post-processing step for MNLS solutions, where it uses the current-density estimate obtained from the MNE and standardizes or divides each source by its variance, which is due to the actual source variance and variation due to the noisy measurements.

It was found that, sLORETA had exact zero-error localization when reconstructing single sources, in all noise-free simulations although the image was blurred, that is, the maximum of the estimated current-density power matches with that of the exact dipole location. In all noisy simulations, it had the lowest localization errors as compared with MNE [9].

IV. RESULTS

The two source-localization approaches (dipole-fit approach using fixed MUSIC algorithm and CDR approach using MNE and sLORETA algorithms) were applied on only EEG, only MEG, band-pass filtered MEG, and both combined, based on averaged and individual head model of five healthy subjects to find out the correct approach for estimating the sources having the location as an a-priori information. For SEPs & SEFs, the sources are expected to be located in the contralateral side of the applied stimulus. In this study, the stimulus was given on the subject's right hand which implies that the corresponding source location should be on the left posterior bank of the central sulcus.

The steps used for source localization are as follows:

- 1) Detect events based on the stimuli. The stimuli time intervals are not consistent (~ 300 ms) throughout the whole recording. Thus to avoid overlapping of events during detection, -50ms before the start of the stimulus

and +50ms after the end of the stimulus were used to separate them.

- 2) Pre-processing steps like notch filtering to avoid the 50 Hz power line artifact and its harmonics and baseline correction to remove a constant offset from the data were used. For a constant baseline correction, a constant pre-trigger was used to determine for each channel the offset that is subtracted from the data.
- 3) Average the pre-processed detected events. The noise level was estimated during the 40ms prestimulus period, which is the region considered as noise for SNR calculation.
- 4) Define the ground truth signal interval for the source analysis, that is, the interval where the N20-peak is clearly seen in the selected channels of EEG and MEG that are located on the left posterior bank of the central sulcus.
- 5) Perform PCA/ICA analysis to determine the number of dipoles, depending on the SNR values ($\text{SNR}'s > 1$), that are used for the dipole-fit algorithm (fixed MUSIC). PCA/ICA filtering was applied to remove the deselected components from the measured data that are obtained after PCA/ICA decomposition, which were considered as noise ($\text{SNR}'s < 0.9$).
- 6) Finally, perform the dipole-fit algorithm on individual and averaged head models and apply CDR algorithms on the individual head models.

The consistency of localization was quite variable from subject to subject as can be seen from table 1. Comparison of source locations are done using visual inspection.

TABLE I
NUMBER OF SUBJECTS THAT SHOWED THE CORRECT ESTIMATES OF THE SOURCE FOR THE INDIVIDUAL AND AVERAGED HEAD MODEL USING DIPOLE (FIXED MUSIC) AND CDR (MNE AND sLORETA) SOURCE ANALYSIS.

	EEG	MEG	MEG_BP	EEG+MEG
Dipole-Individual	3	3	5	3
Dipole-Averaged	3	4	5	3
MNE-Individual	4	1	5	2
sLORETA-Individual	3	1	5	2

In the dipole analysis, both the averaged and the individual head models resulted in almost the same number of subjects that showed the correct estimates of the source. In the CDR analysis, both MNE and sLORETA gave almost the same results. The effect of MEG on EEG is also observed during the combined analyses where the number of subjects showing correct estimates of the source decreases from four to two when using MNE and from three to two when using sLORETA. In both dipole and CDR analysis, the result for MEG shows an improvement after being band-pass (25-330 Hz) filtered, where all five subjects showed correct estimates of the source.

Schematically, the results obtained for one of the representative subjects using dipole and CDR algorithms are shown in Fig. 1 and Fig. 2, respectively.

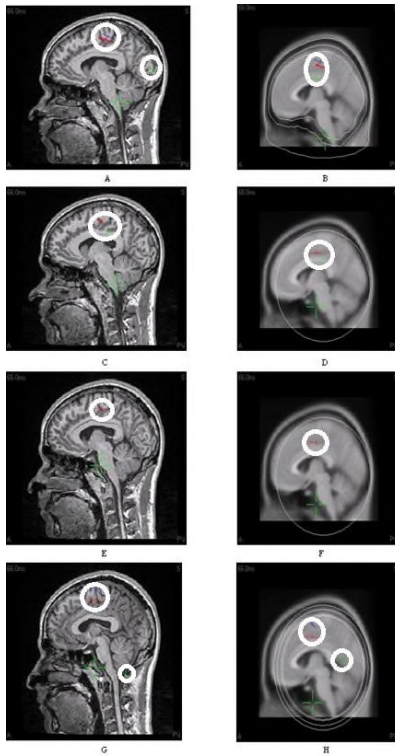


Fig. 1. Single slice plot showing the location of the sources, indicated inside the circles, using dipole fit analysis for EEG only based on A: realistic and B: 3-shell spherical; MEG only based on C: realistic and D: spherical; band-pass filtered MEG based on E: realistic and F: spherical; and both combined based on G: realistic and H: 4-shell spherical head model respectively.

V. CONCLUSIONS

We have analyzed the electric and magnetic localization of the N20 dipole source relative to the individual anatomy and averaged head model. In addition to comparing the different source-analysis algorithms, the differences between two forward head-modeling techniques, namely, a boundary element method and a locally fitted-sphere approach were also compared. In conclusion, as was expected, the dipole analysis, where both the averaged and the individual head models resulted in almost similar result, showed better results than current-density-reconstruction algorithms. An effect of MEG on EEG is observed during combined analyses when using CDR algorithms, due to the software limitation which does not enable us to perform the band-pass filtering separately on the MEG data when analyzing both EEG and MEG.

ACKNOWLEDGMENT

Support from the German Research Council (Deutsche Forschungsgemeinschaft, DFG, SFB 855, Project D2) is gratefully acknowledged.

REFERENCES

- [1] Allison T., McCarthy G., Wood C.C., Jones S.J., Potentials evoked in human and monkey cerebral cortex by stimulation of the median nerve. A review of scalp and intracranial recordings, *Brain*, Vol. 114, No. 6, 1991, pp. 2465-2503.
- [2] Desmedt J.E., Physiology and physiopathology of somatic sensations studied in man by the method of evoked potentials, *Journal of Physiology (Paris)*, Vol. 82, No. 2, 1987, pp. 64-136.

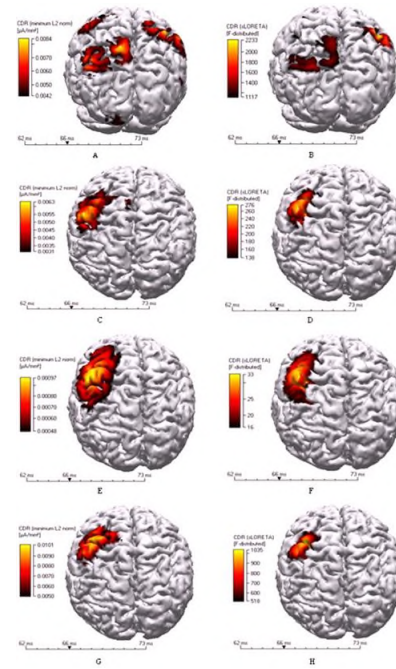


Fig. 2. Cortical surface showing the location of the source for A: EEG only using MNE, B: EEG only using sLORETA, C: MEG only using MNE, D: MEG only using sLORETA, E: MEG_BP using MNE, F: MEG_BP using sLORETA, G: Both combined using MNE and H: Both combined using sLORETA analysis. The bar shows the intensity level of the current density from the lowest to the highest level for MNE and for sLORETA, it shows the statistical distribution. The time bar indicates the selected time range used for the whole analysis and all displayed results are at 66ms which indicates the location of the N20 peak.

- [3] Buchner H., Scherg M., Analysis of the generators of early cortical somatosensory evoked potentials (N. medianus) using dipole source analysis: initial results, *EEG EMG Z Elektroenzephalogr Elektromyogr Verwandte Geb.*, 1991, Vol. 22, No. 2, pp. 62-69.
- [4] Schimpf, P.H., Ramon, C., Hauelsen, J., Dipole models for the EEG and MEG, *Biomedical Engineering, IEEE Transactions on* 49, 2002, pp. 409-418.
- [5] Meneghini F., Vatta F., Esposito F., Mininel S., Di Salle F., Comparison between realistic and spherical approaches in EEG forward modeling, *Biomedizinische Technik, Biomedical engineering*, Vol. 55, 2010, pp. 133-146.
- [6] Jukka Sarvas, Basic mathematical and electromagnetic concepts of the biomagnetic inverse problem, *Physics in Medicine and Biology*, Vol. 32, No. 1, 1987, pp. 11-22.
- [7] Aine, C., Huang, M., Stephen, J., Christner, R., Multistart Algorithms for MEG Empirical Data Analysis Reliably Characterize Locations and Time Courses of Multiple Sources, *NeuroImage* 12, 2000, pp. 159-172.
- [8] Komssi, S., Huttunen, J., Aronen, H.J., Ilmoniemi, R.J., EEG minimum-norm estimation compared with MEG dipole fitting in the localization of somatosensory sources at S1, *Clinical Neurophysiology* 115, 2004, pp. 534-542.
- [9] Grech R., Cassar T., Muscat J., Camilleri K.P., Fabri S.G., Zervakis M., Xanthopoulos P., Sakkalis V., Vanrumste B., Review on solving the inverse problem in EEG source analysis, *Journal of NeuroEngineering and Rehabilitation*, Vol. 5, 2008, pp. 1-25.
- [10] CURRY User Guide, Compumedics USA, Ltd..
- [11] Fuchs, M., Wagner, M., Khler, T., Wischmann, H.A., Linear and Nonlinear Current Density Reconstructions, *Journal of Clinical Neurophysiology*, Vol. 16, No. 3, 1999, pp. 267-295.